The distribution of emission measure, and of heating budget, among the loops in the corona.

G. Peres[1,2], S. Orlando[3], and F. Reale[1]

[1] Dipartimento di Scienze Fisiche ed Astronomiche, Sezione di Astronomia, Piazza del Parlamento 1, 90134 Palermo, Italy;

[3] Osservatorio Astronomico di Palermo, Piazza del Parlamento 1, 90134 Palermo, Italy

R. Rosner

Depts. of Astronomy & Astrophysics and Physics and Enrico Fermi Institute, The University of Chicago; Chicago, Illinois, USA

Received _____; accepted _____

[2]e-mail: peres@oapa.astropa.unipa.it

ABSTRACT

The aim of this paper is to validate a methodology for connecting the emission measure of individual solar coronal loops to the integrated emission measure of the entire solar corona, and using this connection to deduce the energetic properties of the corona, and then to show how this methodology can be applied to observations of solar-like stellar coronae. The solar validation is carried out by using spatially resolved X-ray observations of the Sun obtained from the *Yohkoh* satellite. This work is a further step in our effort to place the "solar-stellar connection" on a quantitative footing. In particular, we show how this analysis procedure can be used in the context of archival *Einstein*, *ROSAT* and EUVE data, as well as Chandra and XMM Newton data, as a complementary analysis tool to existing multi-thermal component models.

Subject headings: coronae: Sun, stars, X-ray observations

1. Introduction

One of the core questions of stellar coronal physics is what determines the intensity of both local heating of particular coronal structures and the overall heating of the corona taken as a whole. In order to answer this sort of question, one must look to both the Sun and other (solar-like) stars: the Sun cannot tell us how the overall heating rate of a stellar corona depends on the presumed "control parameters" (viz., stellar rotation) since most of them are fixed, while in the absence of spatially resolved observations, stars cannot inform us directly about local heating processes. This point has motivated us in a series of recent papers to examine how one might go about comparing solar and stellar observations of what is presumably the same process – the "mechanical" heating of stellar surface layers to produce an X-ray emitting atmosphere (Peres, Orlando, Reale, Rosner, & Hudson, 1997, 2000, Paper II; Orlando, Peres, & Reale 2000a; Paper I). The purpose of the present paper is to extend this work by showing how our detailed understanding of the energetics of individual solar coronal structures can be used to understand the energy budget of solar-like stellar coronae.

The starting point of our analysis is the recognition that the X-ray emitting solar corona appears to be entirely formed by plasma magnetically confined in "loops" (Vaiana et al. 1973), and that while the emission from these loops can fluctuate substantially (e.g., Sheeley & Golub 1979; Shimizu & Tsuneta 1997), this emission is sufficiently steady on the relevant sound crossing and radiative cooling times that simple hydrostatic models suffice to describe them most of the time. Although the phenomenology of these coronal plasma structures seems to be well understood, their heating mechanism remains one of the riddles of coronal physics. Nevertheless, existing spatially resolved observations are able to tell us about the overall energetics of these structures, and to relate it to the ambient magnetic fields (Vaiana & Rosner, 1978; Title & Schrijver, 1998). A central role in our present

discussion will be played by the piece-wise integrated emission measure of individual loops,

$$\mathrm{em}(T) \equiv \int_{T}^{T+\Delta T} q(T')\ dT' \ , \tag{1}$$

where $q(T)$ is the differential emission measure, defined as

$$q(T) \equiv n^2 \left(\frac{dT}{ds}\right)^{-1} \ , \tag{2}$$

n is the plasma density, s is a coordinate along the line-of-sight to the coronal source, $(T_{\rm min}, T_{\rm max})$ is the temperature interval within a given loop over which we integrate the coronal emission, and $T_{\rm max}$ is the loop temperature maximum. We shall assume (with little loss of generality) that the minimum temperature relevant to X-ray emitting loops ($T_{\rm min}$) is the same for all quasi-steady loops. The emission measure has been long known to be a highly useful observationally-constrained quantity for discussing the energetics of stellar atmospheres[2] (e.g., Athay 1966, Jordan 1980). What makes the global emission measure especially useful is the fact that the total solar EM often does not change significantly over time scales of 30 minutes or more (Orlando et al. 2000b), with the obvious exception of flares and similar rapidly evolving, large transients. This observation agrees with the notion that the global emission measure for the coronal X-ray emitting matter, EM, is dominated by the steady X-ray emitting loops.

[2]It is important to recognize that while the emission measure is useful for discussions of the overall energetics, its use is limited for discussions of detailed heating mechanisms: the latter type of discussion requires knowledge of the actual local plasma density, which is not available as long as the spatial substructuring of solar coronal loops remains observationally unconstrained.

Our plan is then as follows: following Paper I and Paper II, we will first discuss the emission measure of individual solar coronal loops in the specific context of *Yohkoh* X-ray images (§II), and show how these individual emission measures can be simply summed by taking advantage of elementary analytical properties of loop emission measures to obtain the overall coronal emission measure. Finally, demonstrate how properties of this integrated emission measure can be used to make deductions about the heating of the loop structures themselves (§III). This lattermost step then allows us to apply our analysis to the spatially unresolved observations of solar-like stellar coronae (§IV).

2. Connecting the global coronal emission measure with the emission measure of single loop structures

The standard Yohkoh data analysis yields pixel maps of temperature and of emission measure from the ratio of two images taken with different filters. From those maps one derives the global distribution of emission measure versus temperature, EM(T): one divides the temperature range into bins of width ΔT, and sums the emission measure of all the pixels belonging to the same temperature bin (Papers I, II). The EM(T) distribution is then the emission measure of the plasma at temperature T summed over the temperature range ΔT, or (similar to Eq. 1)

$$\mathrm{EM}(T) = \int_{T}^{T+\Delta T} Q(T')\ dT'\ , \tag{3}$$

where $Q(T)$ is defined as in Eq. (2); we shall assume that T varies in the range $(T_{\rm min}, T_{\rm Max})$, where $T_{\rm min}$ is the minimum temperature of material within loops contributing to X-ray emission, and $T_{\rm Max}$ is the maximum value of all values of the loop maximum temperature $T_{\rm max}$,

$$T_{\rm Max} \equiv \max\{T_{\rm max}\}\ . \tag{4}$$

It is worth noting that $Q(T)$ is a presumably smooth, continuous, function while EM(T) is a discretized function in the form of a histogram. In our analysis we take $\Delta \log T$ constant, with 29 bins in the range $5.5 \leq \log T(\mathrm{K}) \leq 8$, the nominal range of Yohkoh/SXT, i.e., $\Delta \log T = 2.5/29 \sim 0.09$. Since $\Delta \log T$ is small, we approximate $\Delta T \approx T \Delta \log T \ln 10 \approx \eta T$, with $\eta \approx 0.2$. In this section, we shall connect the emission measure distribution EM(T) to the distribution of emission measures for individual loops.

2.1. The emission measure distribution for an individual loop

First, let us turn to the emission measure of individual loops. We recall from earlier work (viz., Rosner, Tucker and Vaiana, 1978, in the following RTV; Maggio and Peres 1996) that the functional dependence of the emission measure of individual loops, *em*, on temperature depends only on the maximum temperature of the given loops, apart from a (normalizing) multiplicative factor; furthermore, we recall that the emission measure of an individual steady loop, em(T), and the ascending part of the global emission measure, EM(T), of the entire solar corona both obey a simple power law temperature dependence, starting from the minimum temperature (T_{min}), of the form

$$T^{3/2} \ . \tag{5}$$

In the case of the global emission measure, this was already recognized by Athay (1966; also Jordan 1980, Ventura et al. 1998), while Jordan (1980) – studying the very same emission measure – conjectured that EM(T) may be interpreted as due to the sum of contributions from many individual loops. More recently Laming, Drake and Widing (1995) have derived the whole solar disk using the EUV data collected by Malinovsky and Heroux (1973); the emission measure they derive is fully consistent with the above functional form.

The analysis to follow below shows not only that Jordan (1980) was correct, but that this synthesis procedure can be inverted in order to derive the properties of the underlying contributing loops from the integral (global) emission measure. Finally, we note that while the emission measure em(T) of an individual loop terminates at the maximum loop temperature $T_{\rm max}$, the global EM(T) continues for temperatures beyond that at which its maximum value is attained, with a functional form that also can be approximated by a power law of the form

$$T^{-n} \ , \tag{6}$$

where n is typically much larger than 3/2.

Let us now consider the synthesis of individual loop emission measures. For convenience, we write the differential emission measure for a given loop as

$$q(T) = bT^{\gamma} \ ; \tag{7}$$

numerical solutions of the one-dimensional hydrostatic loop equations show that this power law scaling (with $\gamma \approx 1/2$) holds well except for loops whose length far exceeds their scale height, or for loops with highly non-uniform local heat deposition. Since we shall not concern ourselves with these more complex circumstances (see below), we can use this power law relation to integrate as follows:

$$\mathrm{em}(T) = \int_{T}^{T+\Delta T} bT'^{\gamma} \ dT' = \frac{b}{\gamma+1} T^{\gamma+1} \left((1+\eta)^{\gamma+1} - 1 \right) \sim b\eta T^{\gamma+1} \ . \tag{8}$$

Since $T_{\rm max}$ is the maximum loop temperature, we have from the above equation, $\mathrm{em}(T_{\rm max}) = b\eta T_{\rm max}^{\gamma+1} = bT_{\rm max}^{\gamma} \eta T_{\rm max} = q(T_{\rm max}) \eta T_{\rm max}$. In our specific treatment, $\mathrm{em}(T) \propto T^{\beta} \sim T^{3/2}$; thus we find $\gamma = 1/2$, so that the differential emission measure $q(T)$ for a given loop can be expressed in terms of the em($T_{\rm max}$),

$$q(T) = bT^{\gamma} = \frac{\mathrm{em}(T_{\max})}{\eta T_{\max}} \left(\frac{T}{T_{\max}}\right)^{\beta-1} = \frac{\mathrm{em}(T_{\max})}{\eta T_{\max}} \left(\frac{T}{T_{\max}}\right)^{1/2} \tag{9}$$

2.2. The emission measure distribution of loops with the same maximum temperature

As pointed out by many earlier authors, most of the X-ray emission from the solar corona comes from plasma that lies within a (coronal) pressure scale height of the surface; and since most coronal loops appear to have lengths that are equal to, or less than, the pressure scale height corresponding to their maximum temperature, this also means that the bulk of coronal X-ray emission derives from loops with size less than a pressure scale height. (This is not to say that loops that violate these conditions do not exist: such loops do exist, but we argue that they do not make a significant contribution to the integrated coronal X-ray flux.)

As a consequence, we can take advantage of an extremely useful fact about loops with roughly constant pressure: the one-dimensional equations governing the physics of hydrostatic loops of this type are invariant under changes of the loop field-line spatial scale (RTV; Maggio & Peres 1996), so that – aside from a possible multiplicative constant factor – the functional dependence of the loop emission measure distribution versus temperature, $\mathrm{em}(T)$, does not depend on the loop length, but only on the loop maximum temperature $T_{\max}$. Thus, adding the loop emission measures for two or more loops with the same maximum temperature yields exactly the same functional form versus temperature, apart from the normalization.

With this enormous simplification, we can group all loops of the same maximum temperature $T_{\max}$ together, irrespective of their length (and plasma pressure); this group

may be called a $T_{\max}$-equivalence class of loops (obviously indexed by the maximum loop temperature for that equivalence class). Note that, since the product *plasma pressure* × *loop length* determines the coronal temperature (RTV), loops with very different pressure and length may belong to the same $T_{\max}$ equivalence class. Thus, we can use the results of the previous subsection, Eqs. (8) and (9), to write the emission measure for the entire equivalence class of loops with a given maximum temperature $T_{\max}$, $\mathrm{Em}(T_{\max})$, in the form

$$\mathrm{Em}(T,\ T_{\max}) = q_M\ (T/T_{\max})^{\beta}\ , \tag{10}$$

where q_M is the normalizing factor for the emission measure (the maximum value, occurring at $T = T_{\max}$), and β is always approximately 3/2. We have also written $\mathrm{Em}(T,\ T_{\max})$ to state explicitly its dependence on both T and T_{max}.

2.3. Summing the emission measure of all coronal loops

We now model the emission measure of the entire corona as the sum of a multitude of static loops of different maximum temperature. If we define $f(T_{\max})\ dT_{\max}$ as the probability that a loop has a maximum temperature $T_{\max}$, such that $\int f(T_{\max})\ dT_{\max} = 1$, and N is the total number of loops[3], then the emission measure vs. T of all the loops of equal maximum temperature $T_{\max}$, $\mathrm{Em}(T, T_{\max})$, is given by

$$\mathrm{Em}(T, T_{\max}) = N f(T_{\max})\ em(T_{\max})\ (T/T_{\max})^{3/2}, \tag{11}$$

i.e., it too is proportional to $T^{3/2}$ up to the temperature maximum; the corresponding maximum emission measure is thus $N\ f(T_{\max})\ em(T_{\max})$.

[3]Equivalently one may formulate the entire treatment in terms of the amount of solar surface covered by the loops with temperature maximum $T_{\max}$ and emission measure of the loop per unit area, but this would not allow us to disentangle the dependence on pressure (or length) from the area.

The overall emission measure of the corona is due to the sum of all equivalence classes of $T_{\max}$ loops present in the corona up to the largest coronal temperature, here for simplicity indicated as ∞; this is simply

$$\mathrm{EM}(T) = \int_T^{\infty} dT_{\max}\ N\ f(T_{\max})\ em(T_{\max})\ (T/T_{\max})^{\beta}\ . \tag{12}$$

Thus, the global emission measure at temperature T is the sum of the emission measure of all the loops whose maximum temperature $T_{\max} \geq T$. Fig. 1 shows an idealized example of such a sum for a distribution of loops with different $T_{\max}$: we hypothesize a simplified coronal loop population made of six different equivalence classes and derive their EM(T) from Eq. 12. Since the contribution of each $T_{\max}$ loop equivalence class is $\propto T^{\beta}$, the total emission measure distribution is also $\propto T^{\beta}$, up to the lowest value of $T_{\max}$ of all the loop equivalence classes. This will be proved more precisely in the following. The inset of Fig. 1 shows the $N\ f(T_{\max})\ em(T_{\max})$ of the six loop equivalence classes used for this example. More generally, the shape of the global emission measure distribution is determined by the relative contribution of each equivalence class of loops to the overall emission measure (Drake et al. 2000). For example, while the EM(T) distribution of the Sun has, typically, only one maximum, the EM(T) distribution of very active stars may show two maxima (e.g., Griffiths & Jordan 1998). We will comment on this point in the last section.

2.4. The coronal EM(T) derived from observations of the solar corona

Fig. 2 shows the EM(T) derived from a coronal observation made with Yohkoh/SXT. The ascending part of the curve, up to its peak, at the temperature $T_P \approx 2 \times 10^6$ K, is reasonably well approximated by a $T^{3/2}$ power law (cf. also Papers I, II, and Orlando et al. 2000b) up to the peak value, EM_P ($\approx 3.5 \times 10^{49}$ cm^{-3}). This power law behavior

for the ascending part of the emission measure is present in most phases of the solar cycle; Paper II and Orlando et al. (2000b) show several examples of this behavior. If one examines the entire set of Yohkoh/SXT observations along the solar cycle, one finds that T_P varies only by a small factor, while the amplitude of the emission measure at $T = T_P$, $EM_P = EM(T_P)$, varies by several orders of magnitude; both these variations are larger at the time of solar maximum.

For $T > T_P$, the emission measure declines, and again closely follows a single power law of the form $T^{-\alpha}$, with $\alpha \sim 3.5$ (Fig. 2). This behavior holds for all cases of the quasi-steady solar corona that we have studied, although the power law index α varies as the cycle proceeds: α is larger (steeper power law) near solar minimum (cf. Paper II). The close resemblance between the synthetic emission measure distribution shown in Fig. 1 and the observationally-derived emission measure distribution shown in Fig. 2 suggests strongly that the observed distribution can indeed be regarded as a result of the superposition of quasi-static loops characterized by a distribution of maximum loop temperatures; in the following, we will then simply presume that this is indeed the case.

2.5. Deriving the contribution of the various loop equivalence classes

We now show how the contribution of each equivalenced class of loops, e.g., the unknown expression $N\ f(T_{\rm max})\ em(T_{\rm max})$ appearing in Eq. (12), can be recovered from an analysis of the observed EM(T): in Appendix A we show that this expression can be obtained by using Eq. 12 to give

$$N\ f(T_{\rm max})\ em(T_{\rm max}) = \beta \frac{{\rm EM}(T_{\rm max})}{T_{\rm max}} - \frac{d\ {\rm EM}(T_{\rm max})}{dT_{\rm max}}\ . \qquad (13)$$

Now, since

$$\mathrm{EM}(T) \approx \begin{cases} \mathrm{EM}_M \left(\dfrac{T}{T_P}\right)^{\beta} & \text{for } T \leq T_P \\ \\ \mathrm{EM}_M \left(\dfrac{T}{T_P}\right)^{-\alpha} & \text{for } T > T_P \end{cases} \tag{14}$$

we obtain immediately

$$N f(T_{\max})\ em(T_{\max}) \approx \begin{cases} 0 & \text{for } T_{\max} < T_P \\ \\ (\alpha+\beta)\dfrac{\mathrm{EM}_M}{T_P}\left(\dfrac{T_{\max}}{T_P}\right)^{-(\alpha+1)} & \text{for } T_{\max} > T_P \end{cases} \tag{15}$$

The dashed line in Fig. 3 shows the function $Nf(T_{\max})em(T_{\max})$ derived from the emission measure distribution EM(T) shown in Fig. 2, i.e. computed from Eq. 15 with $\beta = 1.5$ and $\alpha = 3.5$. Eq. 15 and Fig. 3 show that $N\ f(T_{\max})\ em(T_{\max})$ is a sharply peaked function around T_P, that there are no (or, more realistically, just very few) loops with $T_{\max} < T_P$, and that the distribution itself decreases for $T_{\max} >\ T_P$ as a power law whose index is smaller by one (i.e., is steeper) than that of EM(T).

Fig. 3 also shows the results of an analysis of the EM(T), using Eq. 13 but taking into account the departure from power laws of the ascending and of the descending parts of EM(T), and considering the effect of error bars and the inherently non-linear characteristics of the analysis. We have made a Monte-Carlo calculation as follows: first for each data point of EM(T) we have generated a random value from a Gaussian distribution centered on the value itself with σ given by the error bar; then applying Eq. 13 to this new EM(T) distribution we obtain a $N\ f(T_{\max})\ em(T_{\max})$. We have thus repeated the Monte-Carlo calculation 1000 times and determined, for each T_{max}, the median value (marked with a diamond) and the bounds enclosing 68% and 90% of the distribution of $N\ f(T_{\max})\ em(T_{\max})$ values obtained with the simulation. These two bounds are shown as error bars of different lengths on each point in Fig. 3. The $N\ f(T_{\max})\ em(T_{\max})$ distribution obtained in this way

is remarkably close to the results of Eq. 15, albeit the latter somehow underestimates the contribution of loops in the descending part, especially hot ($T_{max} \approx 10^7$ K) loops, and of loops with $T_{max} \approx 10^6$ K. The results well below 10^6 K are consistent with no significant contribution from soft X-ray emitting loops, however with large error bars.

For the analytical derivation to follow we will use the piecewise power law description made above, for ease of calculation and because it can help us to gain insight into the results. Also, we will discuss again the limits of our approximations for $T_{\rm max} < T_P$ in the last section.

As an aside, we note (from Eq. (11)) that each equivalence class of loops with the same maximum temperature $T_{\rm max}$ will contribute to the *total* emission measure as follows:

$$\begin{aligned} {\rm Em}_{tot}(T_{\rm max}) &= \int_{T_{\rm min}}^{T_{\rm max}} dT\ N\ f(T_{\rm max})\ em(T_{\rm max})\ \left(\frac{T}{T_{\rm max}}\right)^{\beta} \\ &\approx \frac{\alpha+\beta}{\beta+1}\ {\rm EM}_M\ \left(\frac{T_{\rm max}}{T_P}\right)^{-\alpha} \end{aligned} \tag{16}$$

where $T_{\rm min} \sim 2\times10^5$ K is the lowest coronal temperature we consider, and since $T_{\rm min} \ll T_{\rm max}$ the term containing $T_{\rm min}$ is negligible.

3. Constraints on coronal heating

The fact that EM(T) can be expressed as a sum over the emission measure distribution of many independent static (or quasi-static) loops has important implications on the heating of these structures.

3.1. The heating budget of loops with the same maximum temperature

If $\tilde{\mathrm{Q}}(T)$ is the differential emission measure per unit temperature interval at temperature T of a whole class of loops of the same maximum temperature, $T_{\max}$, and $P(T)$ is the radiative loss per unit emission measure, then the total radiative losses are given by

$$R = \int_{T_{\min}}^{T_{\max}} dT\ \tilde{\mathrm{Q}}(T)\ P(T)\ . \tag{17}$$

Since

$$\tilde{\mathrm{Q}}(T) = N\ f(T_{\max})\ em(T_{\max}) \times \frac{1}{\eta T_{\max}} \left(\frac{T}{T_{\max}}\right)^{\beta-1}\ , \tag{18}$$

in analogy to what was discussed in §2, and $P(T) \approx P_0 T^{-1}$ in the range 2×10^5 K $< T < 10^7$ K, with $P_0 \sim 2.02 \times 10^{-16}$ erg s^{-1} cm^3 K (from the MEKAL spectral model; Mewe, Lemen, & van den Oord 1986; Kaastra 1992; Mewe, Kaastra & Liedahl 1995 and references therein),

$$\begin{aligned} R &= \frac{N\ f(T_{\max})\ em(T_{\max})}{\eta}\ \frac{P_0}{T_{\max}^{\beta}} \int_{T_{\min}}^{T_{\max}} T^{\beta-2}\ dT \\ &\approx \frac{N\ f(T_{\max})\ em(T_{\max})}{\eta(\beta-1)}\ P_0\ T_{\max}^{-1}\ , \end{aligned} \tag{19}$$

where we have neglected $T_{\min}^{\beta-1}$ since $T_{\min} \ll T_{\max}$.

These radiative losses are approximately one half of the total energy input to the loop, the other half being conducted towards the lower transition region, where it is radiated away (cf., Vesecky, Antiochos, & Underwood 1979). The total amount of heat delivered within loops with temperature maximum $T_{\max}$ is thus given by

$$h(T_{\max}) \approx \frac{2}{\eta(\beta-1)}\ N\ f(T_{\max})\ em(T_{\max})\ P_0\ T_{\max}^{-1} \tag{20}$$

Therefore, using Eq. 15

$$h(T_{\max}) \approx \begin{cases} 0 & \text{for } T_{\max} < T_P \\ \\ \dfrac{2(\alpha+\beta)}{\eta(\beta-1)} \dfrac{\mathrm{EM}_M\ P_0}{T_P^2}\ \left(\dfrac{T_{\max}}{T_P}\right)^{-(\alpha+2)} & \text{for } T_{\max} \geq T_P\ . \end{cases} \tag{21}$$

Fig. 4 shows the heating budget $h(T_{\max})$ for each equivalence class of loops characterized by the temperature maximum $T_{\max}$, as derived from the function $Nf(T_{\max})em(T_{\max})$ of Fig. 3; recall that $\beta \approx 3/2$ and that, for the case shown in Fig. 2, $T_P \approx 1.7 \times 10^6$K, $EM_P \approx 3.5 \times 10^{49}$ cm^{-3} and $\alpha \approx 3.5$. Thus, the total coronal loop heating rate up to a reference temperature t is given simply by

$$H(t) \approx 2R = 2 \int_{T_{\min}}^{t} dT\ Q(T)\ P(T)\ . \tag{22}$$

Our aim is now to evaluate this equation for the reference temperature t, and then to allow t to increase indefinitely in order to obtain the total coronal heating rate. On the basis of Eq. 9, $Q(T) = Q_M(T/T_P)^{\xi-1}$, $Q_M = \mathrm{EM}_M/\eta T_P$ and, for generality, we indicate with ξ the index of the power laws in the ascending and in the descending part of $EM(T)$:

$$\xi = \begin{cases} \beta & \text{for } T < T_P \\ -\alpha & \text{for } T > T_P \end{cases} \tag{23}$$

From Eq. 22,

$$H(t) = 2 \int_{T_m in}^{t} dT\ Q(T)\ P(T) = 2\frac{\mathrm{EM}_M}{\eta T_P} \int_{T_m in}^{t} \left(\frac{T}{T_P}\right)^{\xi-1} P(T)\ dT = 2\frac{\mathrm{EM}_M}{\eta T_P} P_0 \int_{\tau_m in}^{\tau'} \tau^{\xi-2} d\tau \tag{24}$$

where $\tau = T/T_P$, $\tau_{\min} = T_{\min}/T_P$, $\tau' = t/T_P$, and

$$H(t) = \frac{2\mathrm{EM}_M P_0}{\eta T_P} \times \begin{cases} \dfrac{(t/T_P)^{\beta-1} - (T_{\min}/T_P)^{\beta-1}}{\beta - 1} & \text{for} \quad t \le T_P \\ \dfrac{1 - (T_{\min}/T_P)^{\beta-1}}{\beta - 1} + \dfrac{1 - (t/T_P)^{-(\alpha+1)}}{\alpha + 1} & \text{for} \quad t > T_P \end{cases} \tag{25}$$

which for $t \gg T_P$ yields the total heating budget

$$H_{tot} = \frac{2\mathrm{EM}_M P_0}{\eta T_P} \left[\frac{1 - (T_{\min}/T_P)^{\beta-1}}{\beta - 1} + \frac{1}{\alpha + 1}\right] \tag{26}$$

and for $T_{\min} \ll T_P$

$$H_{tot} \approx \frac{2\mathrm{EM}_M P_0}{\eta T_P} \left(\frac{1}{\beta - 1} + \frac{1}{\alpha + 1}\right)\ . \tag{27}$$

Fig. 5 shows the curve $H(t)$ for the emission measure distribution $EM(T)$ of Fig. 2. The above equation shows that the entire coronal heating budget is approximately proportional to the peak value of the emission measure distribution (EM_P), and inversely proportional to the temperature of maximum emission measure (T_P), with a rather mild dependence on the indices of the ascending and descending power laws, β and $-\alpha$, respectively, which just enter via the factor

$$\frac{2}{k}\left(\frac{1}{\beta-1}+\frac{1}{\alpha+1}\right) \ ; \tag{28}$$

the value of this factor is approximately 20 for the specific case shown in Fig. 2.

For the specific case shown in Fig. 2, $H_{tot} \approx 9.6 \times 10^{28}$ ergs s^{-1}, i.e., approximately twice the total radiative losses we found in paper II for the same emission measure distribution; this is of course not a surprise since we built in this fact in our assumption regarding the evaluation of H immediately preceeding Eq. 20.

3.2. Average heating rate per unit volume within loops

The total heat deposited in a set of loops characterized by maximum temperature $T_{\max}$ can also be expressed as

$$h(T_{\max}) = \sum_j E_{Hj}\ L_j\ a_j \ , \tag{29}$$

where E_{Hj} is the average heating rate per unit volume, assumed uniform inside the loop for simplicity, a_j is the area covered by the two footpoints on the solar (or stellar) surface and L_j is the semilength of the loops with $T_{\max}$ as temperature maximum. The index j runs over all loops with maximum temperature $T_{\max}$.

We now consider the two scaling laws for the plasma confined inside a hydrostatic loop (RTV):

$$T_{\max} = 1.4 \times 10^3 (pL)^{1/3} \tag{30}$$

$$E_H = 10^5 \; p^{7/6} \; L^{-5/6} \tag{31}$$

where p is the coronal pressure (by assumption, essentially constant within loops shorter than the pressure scale height), and E_H is the average coronal heating per unit volume inside such loops. These equations allow us to solve for the pressure in terms of the loop length and maximum temperature,

$$p = \frac{1}{L} \left(\frac{T_{\rm max}}{1.4 \times 10^3} \right)^3 \tag{32}$$

and, upon substituting Eq. 32 into Eq. 31, one obtains

$$E_H = \begin{cases} 0 & \text{for } T_{\rm max} < T_P \\ \\ 10^5 \left(\dfrac{T_{\rm max}}{1.4 \times 10^3} \right)^{7/2} \; L^{-2} & \text{for } T_{\rm max} \geq T_P \; . \end{cases} \tag{33}$$

where we have taken into account the fact that, in practice, very few loops exist with $T_{\rm max} < T_P$. We can now solve for L for $T_{\rm max} \geq T_P$ from the above equation, and substitute into Eq. 29 to obtain, for $T_{\rm max} \geq T_P$

$$h(T_{\rm max}) = 9.9 \times 10^{-4} \; T_{\rm max}^{7/4} \sum_j E_{Hj}^{1/2} \; a_j \approx 10^{-3} T_{\rm max}^{7/4} \sum_j E_{Hj}^{1/2} \; a_j \; . \tag{34}$$

Since this expression does not depend on L, it therefore applies to all loops with the same maximum temperature $T_{\rm max}$. Equating the right-hand sides of this equation and Eq. 21, for $T_{\rm max} \geq T_P$

$$\frac{2(\alpha+\beta)}{\eta(\beta-1)} \frac{{\rm EM}_M \; P_0}{T_P^2} \left(\frac{T_{\rm max}}{T_P} \right)^{-(\alpha+2)} = 10^{-3} T_{\rm max}^{7/4} \sum_j E_{Hj}^{1/2} \; a_j \tag{35}$$

therefore

$$\sum_j E_{Hj}^{1/2} \; a_j = \begin{cases} 0 & \text{for } T_{\rm max} < T_P \\ \\ 2 \times 10^3 \left[\dfrac{EM_P P_0}{\eta} \dfrac{\alpha+\beta}{\beta-1} {T_P}^{\alpha} \right] T_{max}^{-(\alpha+3.75)} & \text{for } T_{\rm max} \geq T_P \; . \end{cases} \tag{36}$$

For the EM($T_{\rm max}$) shown in Fig. 2, $\alpha \approx 3.5$; using the typical value $\beta = 1.5$, we find that

$$\sum_j E_{Hj}^{1/2}\ a_j = \begin{cases} 0 & \text{for } T_{\rm max} < T_P \\ \\ 2\times 10^4 \left[\dfrac{EM_P P_0}{\eta} {T_P}^{3.5}\right] T_{\rm max}^{-7.25} & \text{for } T_{\rm max} \geq T_P\ . \end{cases} \tag{37}$$

Fig. 6 shows, as an example, the expression $\sum_j E_{Hj}^{1/2}\ a_j$ corresponding to the emission measure distributions EM($T_{\rm max}$) of Fig. 2.

Now, in order to derive the volumetric heating rate E_H one needs to know the coefficients $\{a_j\}$ which, however, cannot be derived from the emission measure itself, nor can they be derived from stellar observations.

Finally, we note that the power law dependence on $T_{\rm max}$ in Eq. 37 is rather steep. However, common experience with coronal loops shows that hotter loops (higher $T_{\rm max}$) are more intensely heated (higher E_H), so that $E_H \propto T_{\rm max}^{\zeta}$ with $\zeta > 0$; thus we can conjecture that the steep power law dependence in Eq. 37 mostly reflects the dependence of a_j on $T_{\rm max}$, i.e., that $a_j(T_{\rm max}) \propto T_{\rm max}^{-7.25}$ or even steeper. Equivalently, one may substitute E_H from Eq. 33 into 29 to obtain

$$h(T_{\rm max}) = \begin{cases} 0 & \text{for } T_{\rm max} < T_P \\ \\ 10^5 \left(\dfrac{T_{\rm max}}{1.4\times 10^3}\right)^{7/2} \displaystyle\sum_j \frac{1}{L_j^2} L_j a_j = 9.7\times 10^{-7} T_{\rm max}^{7/2} \sum_j \frac{a_j}{L_j} & \text{for } T_{\rm max} \geq T_P\ . \end{cases} \tag{38}$$

This equation shows explicitly the link between the heating budget and the geometrical factors. It may at first sight appear that there is no dependence on parameters such as the plasma pressure; these are, however, involved through the scaling laws and their dependence on L.

Appendix B presents an evaluation of the heating of loops with $T_{\rm max} \approx 2\times 10^6$K

in order to provide the reader with a feeling of the orders of magnitude involved in this discussion.

4. Discussion and conclusions

We have studied the piecewise-integrated emission measure versus temperature, $EM(T)$, of the solar corona taken as a whole, i.e., as if it were an unresolved stellar corona. Using the facts that the corona is almost entirely composed of steady loops whose height is less than their pressure scale height and that the emission measure distribution versus temperature for each static loop is $\propto T^{\beta}$ (with $\beta \approx 1.5$), we have found that we can derive the distribution of the emitting loops versus temperature from the emission measure distribution $EM(T)$, as well as the heating budget for loops with different maximum temperature.

Rather than focusing on the energetics of individual loops, this paper studies the solar corona taken as a whole, in the same way that stellar observations treat stellar coronae. In our model of the solar corona, loops with the same maximum temperature $T_{\rm max}$ are grouped together as their emission measure distribution as a function of temperature would be indistinguishable from that of a single loop with the same $T_{\rm max}$ and emission measure equal to the sum of their emission measures. We then sum all the contributions of such "equivalence classes" of loops over $T_{\rm max}$ to obtain the total coronal emission measure distribution. We show further that the observed total coronal emission measure distribution versus temperature, $EM(T)$, agrees with the results of such a model calculation. Furthermore, we show that if one differentiates the observed $EM(T)$ with respect to temperature, one obtains the emission measure for all loops with a given maximum temperature $T_{\rm max}$ present at that time in the corona. This suggests that our method may be directly applied to the stellar case, in which case loop structures cannot be resolved

individually, and it may represent an alternative to the fitting with multiple thermal components for those cases in which the emission measure distribution can be derived.

In a recent work Aschwanden et al. (2000) study coronal loops observed with TRACE; they claim that these loops appear to be isothermal, i.e. very different from the standard scenario given by, for instance, Yohkoh data, of loops dominated by the balance of heating, radiative losses and, more important, thermal conduction.

However, the temperature and emission determination by Aschwanden et al., as the analysis routinely used for TRACE data, is based on narrow band XUV filter ratio method: each of the narrow bands accepts few spectral lines which form at rather different temperatures, i.e. approximately between 10^5 and 10^7 K. As a consequence, the temperature vs. filter-band-ratio is a multi-valued function, and so the relevant temperature determination is not-unique. The solution chosen, for the data analysis routinely used, has been to force the 195/171 AA ratio to be (approximately) in the $0.9 - 1.8 \times 10^6$ K temperature range based on the claim that this is the range of maximum line visibility at constant emission measure. As we discuss below, ignoring the role of emission measure in determining plasma visibility and the fact that loops can have widely different emission measure values, can lead to severe errors.

Indeed, on the basis of coronal loop physics matured over decades of X-ray observations and modeling, it is known that hotter loops have a corresponding much higher pressure and higher emission measure compensating for the presumed lower visibility, as can be easily seen with hydrostatic loop models. Since the entire loop density distribution scales with the loop maximum temperature as T_{max}^2, their emission measure measure should scale as T_{max}^4. Taking this feature into account along with the spectral response of TRACE, loops between 10^6 K and 10^7 K are all almost equally visible, much more visible than presumed in the TRACE data analysis system. The plasma detected in all this wide range is however

invariably assumed to be in the $0.9 - 1.8 \times 10^6$ K range: any thermal structure along the loop is entirely wiped out and all the loops are claimed to be at the same temperature.

Testa et al. (2001a, 2001b) have analyzed some coronal loops observed with TRACE, relaxing the above mentioned limitation of temperature and trying a novel approach to the TRACE data analysis. They have fitted both the brightness profiles in the 171 A and 195 A bands, used for standard TRACE observations, along the loops *and* used the filter ratio values, after removing the background emission. They find that some loops appear to be at 5×10^6 K and not isothermal, while others are consistent with isothermal but at 10^5 K, i.e. more alike some loops observed with SOHO/CDS (Brekke et al., 1997) and S-055 Skylab (Foukal, 1976).

Furthermore, spectroscopic work by Brosius et al. (1986), Raymond and Doyle (1981), Jordan (1980), Laming, Drake and Widing (1995) yield a coronal emission measure typically $\propto T^{3/2}$ and Priest et al. (2000) obtain a good fit of a coronal loop with a not-isothermal profile, assuming an energy balance between a heating term, heat conduction and radiative losses; Priest et al. claim "strong evidence against heating concentrated near the loop base", i.e. opposite to one of the key conclusions of Aschwanden et al. analysis.

Incidentally, Aschwanden et al. (2000) do not show that the loops, claimed to be isothermal, are statistically important - i.e. very frequent - in the overall well proved scenario of hot coronal loops dominated by heat conduction and definitely not-isothermal.

For all these reasons we have decided not to take into account possible "isothermal" coronal loops and consider just the well founded coronal loops scenario based on X-ray photometric observations and UV spectroscopic studies.

The method presented here is substantially different from that of Maggio & Peres (1996), who carry out a "minimum χ^2" fit of stellar low-resolution X-ray spectra with

one- or two-loop coronal models: here instead we model the coronal emission measure distribution as due to a continuum of loops.

Our results show that, aside from times when flares or other large transients dominate coronal emission, the temperature dependence of the emission measure distribution of the entire solar corona can be modeled as a power law of the form $\propto T^{3/2}$, up to a maximum temperature which typically lies between 10^6 K and 2×10^6 K. For $T > T_P$, we show that the emission measure distribution decreases as a steep power law in T. This decrease of EM(T) for $T > T_P$ can be used to derive the distributions both of loops and of their heating as a function of $T_{\rm max}$, the loops' maximum temperature. Finally, we show (on the basis of Eq. 15) that there are relatively few loops with maximum temperature well below T_P; indeed, we show that the distribution of emitting loops, derived on the basis of Eq. 15, and the temperature dependence of the heating rate (Eq. 21) are rather sharp functions of $T_{\rm max}$. An important (as yet unresolved) issue to what extent this sharp temperature dependence is real, rather than depending on (either) a somewhat too idealized model or the unavoidably limited instrumental capabilities of Yohkoh/SXT (in particular, its spectral resolution). Observations using EUV spectroscopic data (e.g., Brosius et al. 1996) show rather similar emission measure distributions, suggesting that the steep rise of the loop distribution is very likely real; nevertheless, it seems extraordinary that there are very few quasi-steady loops with $T_{\rm max} < 1.7 \times 10^6$ K. In any case, it appears reasonable that the contribution of quasi-steady loops with maximum temperature below 1 or 2 million degrees to EM(T) is indeed very small relative to the hotter corona, albeit not exactly zero, at the maximum of the solar cycle.

The largest contribution to the coronal emission measure, to the coronal radiative losses and to the coronal heating is due to loops with maximum temperature around the peak of EM(T). The steep decrease of the solar EM(T) beyond the temperature of maximum

EM(T) implies that loops are fewer and fewer for higher and higher $T_{\max}$, and that less and less total heat is delivered in the hotter loops. This peak evolves as a function of the solar cycle: From Eq. 15, Eq. 21, and from the evolution of EM(T) during the solar cycle (Paper II; Orlando et al. 2000b) we can infer the evolution of the emitting loop distribution and of the related heating distribution. Observations show that both distributions become more concentrated at lower temperatures, and that their maximum value gets smaller during the minimum of the solar cycle; we also know that the ascending, low temperature, portion of EM(T) becomes slightly steeper during the solar minimum. The steepening during the minimum of the cycle may be due to several causes, including the low Yohkoh/SXT sensitivity to cooler plasma or (more likely) to the fact that most of the corona is devoid of loops and thus consist mostly of non-confined plasma. In spite of this, T_P varies only between $\approx 2 \times 10^6$ K and $\approx 7 \times 10^5$ K during the solar cycle.

On the other hand EM(T), T_P and, therefore, the distribution of loop emission measure and heating versus $T_{\max}$ all appear to be subject to negligible (if any) changes on time scales of hours or – sometimes – days (away from flares). The steadiness of EM(T), and therefore of the distributions of the loops and of the heating, over a few hours (Orlando et al. 2000b) seems to imply an analogous steadiness of the heating budget of the entire confined solar corona, with only slow and gradual changes. It is not clear why this is so. One possibility is that this observational characteristic is just a consequence of summing randomly distributed contributions over the entire corona, so that it just reflects the effects of statistical temporal smoothing rather than true steadiness of the entire corona. Another possibility is that the global externally supplied energy budget of the corona is actually steady. Either possibility would have major implications for the heating process of the corona.

Finally, we note that it is straightforward to see from Eq. 13 that any flattening, or even increase, at a given temperature T^* of the emission measure EM(T) along its

descending portion would provide evidence for another preeminent set of loops, and related heating, with $T_{\max} \approx T^*$. In particular, a doubly-peaked EM(T) (as the one found, for instance, by Griffith & Jordan 1998) implies a doubly peaked loop distribution. In the light of our results, the findings of Griffiths & Jordan (1998) are indicative of two distinct distributions of steady loops peaking at two rather different temperatures, one at several 10^6 K and the other at a few 10^7 K. Alternatively, it may be that steady coronal emission is accompanied in some (very active) stars by a relatively large number of simultanteous flares whose light curves overlap in such a way that they mask much – if not all – of the variability (e.g., Giampapa et al. 1996; Paper II); see Reale et al. (2000) and Peres (2000).

Our method allows us – in principle – to infer the global distribution of the heating versus the loop maximum temperature; this information can, in turn, provide constraints on the heating mechanism of the corona and on the global coronal energy budget. On the practical level, however, it is far from easy to derive a relationship between the loops' average volumetric heating rate and the loop temperature as one needs to know the fraction of the solar surface covered by the footpoints of the loops with given maximum temperature $T_{\max}$.

As for future applications, we plan to apply extensively the diagnostics presented here to the EM(T) of the whole solar corona at several points during the solar cycle, using the large data set collected with Yohkoh/SXT. It is also possible to apply the diagnostics to selected portions of the corona, e.g., Yohkoh/SXT data on single active regions, or to SERTS observations (Brosius et al. 1996). The diagnostics can also be modified very easily for application to the diffential emission measure distribution, rather than to the piecewise-integrated emission measure treated here. For obvious reasons, our analysis is well suited to stellar observations since it uses a global coronal characteristics, EM(T), readily obtained by a spectroscopic coronal observation. We foresee an immediate application to

EUVE stellar observations (Drake et al. 2000); and we also plan to apply it to data obtained from the spectroscopic X-ray instruments onboard the Chandra and XMM-Newton X-ray astronomy missions. It will be particularly instructive to compare the results for stars of different activity levels with the analogous solar results.

We acknowledge useful suggestions and comments from S. Serio and E. Franciosini, and useful discussions with C. Kankelborg. We also acknowledge useful suggestions from an anonymous referee. This work has been partially supported by the Agenzia Spaziale Italiana and by the Italian Ministero dell'Università e della Ricerca Scientifica e Tecnologica.

A. Deriving the loop population from EM(T)

Our task is to derive $N\ f(T_{\rm max})\ em(T_{\rm max})$ from the observed EM(T). On the basis of Eq. (12),

$$\frac{d\ {\rm EM}(T)}{dT} = \beta\ T^{\beta-1} \int_T^\infty dT_{\rm max}\ N\ f(T_{\rm max})\ em(T_{\rm max})\ (T_{\rm max})^{-\beta} +$$

$$+ T^\beta\ \frac{d}{dT} \int_T^\infty dT_{\rm max}\ N\ f(T_{\rm max})\ em(T_{\rm max})\ (T_{\rm max})^{-\beta}$$

$$= \beta\ \frac{{\rm EM}(T)}{T} - N\ f(T)\ em(T)$$

since the last term is

$$T^\beta \lim_{\Delta T\to 0} \frac{1}{\Delta T} \left[\int_{T+\Delta T}^\infty dT_{\rm max}\ N\ f(T_{\rm max})\ em(T_{\rm max})\ (T_{\rm max})^{-\beta} - \right.$$

$$
\begin{aligned}
&\left. - \int_T^\infty \; dT_{\rm max} \; N \; f(T_{\rm max}) \; em(T_{\rm max}) \; (T_{\rm max})^{-\beta} \right] \\
&= T^\beta \lim_{\Delta T \to 0} \frac{1}{\Delta T} \int_T^{T+\Delta T} \; dT_{\rm max} \; N \; f(T_{\rm max}) \; em(T_{\rm max}) \; (T_{\rm max})^{-\beta} \\
&= T^\beta \lim_{\Delta T \to 0} \frac{1}{\Delta T} N \; f(T) \; em(T) T^{-\beta} \Delta T \\
&= N \; f(T) \; em(T) \; ,
\end{aligned}
$$

and therefore

$$
N \; f(T) \; em(T) = \beta \; \frac{\rm EM(T)}{T} \quad - \quad \frac{d \; \rm EM(T)}{dT} \; . \tag{A1}
$$

This expression connects the distribution function of loop maximum temperatures to the global emission measure distribution. In the specific case of a $\beta = 3/2$ power law, we obtain instead of Eq. A1

$$
N \; f(T) \; em(T) = \quad \frac{3}{2} \; \frac{\rm EM(T)}{T} \quad - \quad \frac{d \; \rm EM(T)}{dT} \; . \tag{A2}
$$

B. Example: the heating budget of loops with $T_{\rm max} \approx 2 \times 10^6$K

In this appendix, we evaluate the heating budget of loops with $T_{\rm max}$ in the range of 2×10^6K, using a few simple assumptions; our aim is to provide the reader with a feeling of the orders of magnitude involved.

As a first simplification, we note that since loops with $T_{\rm max} \approx 2 \times 10^6$K largely dominate the emission measure distribution, their total emission measure ϵ is comparable to the maximum value of $EM(T)$ and therefore we shall assume $\epsilon \approx 10^{49}$ cm^{-3}. The emission measure in an equivalence class of loops with maximum temperature $T_{\rm max}$ (all with the same length L and, therefore, pressure p) can then be approximated as $\epsilon = \; n_p^2 V = \; p^2 V/(2 k_B T_{\rm max})^2$; n_p is the proton number density, V is the loops' total

volume, and k_B is the Boltzmann constant; according to the RTV loop scaling laws, $T^3_{\rm max} = (1.4 \times 10^3)^3\ p\ L$, and therefore $n_p^2 = T^4_{\rm max}/(bL^2)$, where $b \approx 5.7 \times 10^{-13}$. Thus, upon substitution, we find that the emission measure is given by the expression $\epsilon = T^4_{\rm max} V/(bL^2)$ and $V = \epsilon\ b\ L^2/T^4_{\rm max}$.

However, loops with the same temperature may have different, even very different, lengths. Let us consider, then, for simplicity just two values of L, 10^9 cm and 10^{10} cm, the first representative of active regions loops, the other of more quiet and extended loops but still shorter than the pressure scale height; their total emission measure is $\epsilon_1 + \epsilon_2 = \epsilon$ and their total volume is $V = V_1 + V_2 = b\ (EM_1 L_1^2 + EM_2 L_2^2)/T^4_{\rm max}$ (where, from here on, all quantities with suffixes 1 and 2 pertain to, respectively, the first and the second set of loops). Then if we assume that $V_1 = V_2$, and since $L_1 = 0.1 L_2$, we are led to the result $\epsilon_1 = 100\ \epsilon_2$. If we insert numerical values for the various known quantities, we then obtain $V \approx 10^{30}$ cm^3.

Furthermore we may assume that loops have an aspect ratio $L/r \approx 10$ (a typical value of most loops observed) where r is the cross-sectional radius of the loop. The volume of each loop is then $v = 2\pi r^2 L = 2 \times \pi 0.1^2 L^2 \times L = 0.02\pi L^3$. On the basis of these considerations we would then have n_1 loops for the first set and n_2 for the second, such that $n_1 = V/\ 2v_1 \approx 8 \times 10^3$ loops and $n_2 \approx 8$ loops.

Under the same assumptions, the sum in Eq. (38) can be re-written in the form

$$\Sigma a_j/L_j = \Sigma \pi 0.01 L_j\ , \tag{B1}$$

so that the contribution of all loops with the same length within the $T_{\rm max}$ equivalence class would amount to $n\pi \times 0.01L$. Thus, for the first of loops considered above, $n_1\pi \times 0.01 L_1 = 8 \times 10^3 \pi \times 0.01 \times 10^9 = 2.5 \times 10^{11}$ and $n_2\pi \times 0.01 L_2 = 8\pi \times 0.01 \times 10^{10} = 2.5 \times 10^9$. Evidently under these assumptions the set 1 of loops, i.e., those with $L = 10^9$cm, have a significantly larger sum, and therefore

dominate the heating budget of the $T_{\max}$ equivalence class. Thus, from Eq. (38) we have $h(2 \times 10^6 K) \approx 10^{-6} \times 11.3 \times 10^{21} \times \ 2.5 \times 10^{11} erg \approx 28.3 \times 10^{26}$ erg.

References

Aschwanden, M.J., Nightingale, R.W., & Alexander, D. 2000, ApJ, 541, 1059

Athay, R.G., 1966, ApJ 145, 784

Brekke, P., Kjeldseth-Moe, O., & Harrison, R. A. 1997, Solar Physics, 175, 511

Brosius, J.W., Davila, J.M., Thomas, R.J., & Monsignori–Fossi, B.C., 1996, ApJS, 106, 143

Drake, J.J., Peres, G., Orlando, S., Laming, J.M., & Maggio, A. 2000, ApJ, 545, 1074

Foukal, P.V. 1976, ApJ, 210, 575

Giampapa, M. S., Rosner, R., Kashyap, V., Fleming, T. A., Schmitt, J. H. M. M., & Bookbinder, J. A. 1996, ApJ, 463, 707

Griffiths, N.W., & Jordan, C., 1998, ApJ 497, 883

Jordan, C., 1980, A&A 86, 355

Kaastra, J.S. 1992, An X-Ray Spectral Code for Optically Thin Plasmas (Internal SRON-Leiden Report, updated version 2.0)

Laming, J.M., Drake, J.J., & Widing, K.W. 1995, ApJ443, 416

Maggio, A., & Peres, G., 1996, A&A 306, 563

Malinovsky, M., & Heroux, L., 1973, ApJ181, 1009

Mewe, R., Kaastra, J.S., & Liedahl, D.A. 1995, Legacy, 6, 16

Mewe, R., Lemen, J.R., & van den Oord, G.H.J. 1986, A&AS, 65, 511

Orlando, S., Peres, G., & Reale, F. 2000a, ApJ528, 524 [Paper I]

Orlando, S., Peres, G., & Reale, F. 2000b, in preparation

Peres, G., 2000, Proc. of the "X–Ray Astronomy 2000" meeting, PASP, in preparation

Peres, G., Orlando, S., Reale, F., Rosner, R., & Hudson, H. 1997, in "Observational Plasma Astrophysics: Five Years of Yohkoh and beyond", Watanabe, T., Kosugi, T., Sterling, A.C. eds., Kluwer, p. 29

Peres, G., Orlando, S., Reale, F., Rosner, R., & Hudson, H. 2000, ApJ, 528, 537-551 [Paper II].

Priest, E.R., Foley, C.R., Heyvaerts, J., Arber, T.D., Mackay, D., Culhane, J.L., & Acton, L.W. 2000, ApJ, 539, 1002

Raymond, J.C., & Doyle, J.G. 1981, ApJ, 247, 686

Reale, F., Orlando, S., & Peres, G., et al. 2000, in preparation

Rosner, R., Tucker, W.H., & Vaiana, G.S., 1978, ApJ 220, 643

Sheeley, N., & Golub, L. 1979, Sol. Phys. 63, 119.

Shimizu, T., & Tsuneta, S. 1997, ApJ 486, 1045.

Testa, P., Peres, G., Orlando, S., & Reale, F., 2001 a, in Solar Encounter: the First Solar Orbiter Workshop, ESA Special Publication SP-493, in press

Testa, P., Peres, G., Orlando, S., & Reale, F., 2001 b, in preparation

Title, A., & Schrijver, K. 1998, ASP Conf. Ser. 154, The Tenth Cambridge Workshop on Cool Stars, Stellar Systems and the Sun, Edited by R. A. Donahue and J. A. Bookbinder, p.345

Vaiana, G.S., Krieger, A.S., & Timothy, A.F. 1973, Sol. Phys, 32, 81.

Vaiana, G.S., & Rosner, R. 1978, ARA&A,16, 393-428.

Ventura, R., Maggio, A., & Peres, G., 1998, A&A 334, 188

Vesecky, J.F., Antiochos, S.K., & Underwood, J.H. 1979, ApJ, 233, 987

Fig. 1.— A simple example of summing the piecewise integrated emission measure distribution of various loop equivalence classes (six in this case), of different temperature maxima. The thin lines yield the $T^{3/2}$ contribution of each class of loops having the same $T_{\max}$ and the dotted vertical lines mark the related $T_{\max}$ values. The solid histogram is the sum of all the equivalence classes and is $\propto T^{3/2}$ up to the lowest $T_{\max}$. The inset shows the assumed $Nf(T_{\max})em(T_{\max})$.

Fig. 2.— Piece-wise integrated emission measure distribution for the whole corona, observed with Yohkoh/SXT on 6 Jan 92, at 21:45 UT (top), close to the maximum of the solar cycle.

Fig. 3.— $Nf(T_{\max})em(T_{\max})$ derived from the EM(T) of Fig. 2. Diamonds, error bars and solid connecting line are the results of the Monte-Carlo calculation discussed in the text: diamonds mark the average values, small error tics on the error bars enclose the 68% of the values, the large ones the 90%. The dashed line shows the result in the alternative calculation, approximating the ascending part up to the maximum with a $T^{3/2}$ power law and the descending part with a $T^{-3.5}$ power law, and then applying Eq. 15 to the two power laws.

Fig. 4.— The function $h(T_{\max})$, i.e. the heating budget of each equivalence class corresponding to maximum loop temperature $T_{\max}$.

Fig. 5.— The function $H(t)$, i.e., the heating budget of the whole corona, integrated up to temperature t. The figure shows that most of the contribution occurs for $t \leq T_P$; T_P is where the slope visibly changes.

Fig. 6.— $\sum_j E_{Hj}^{1/2}\ a_j$ for loops with maximum temperature $T_{\max}$, derived from the EM(T) of Fig. 2.

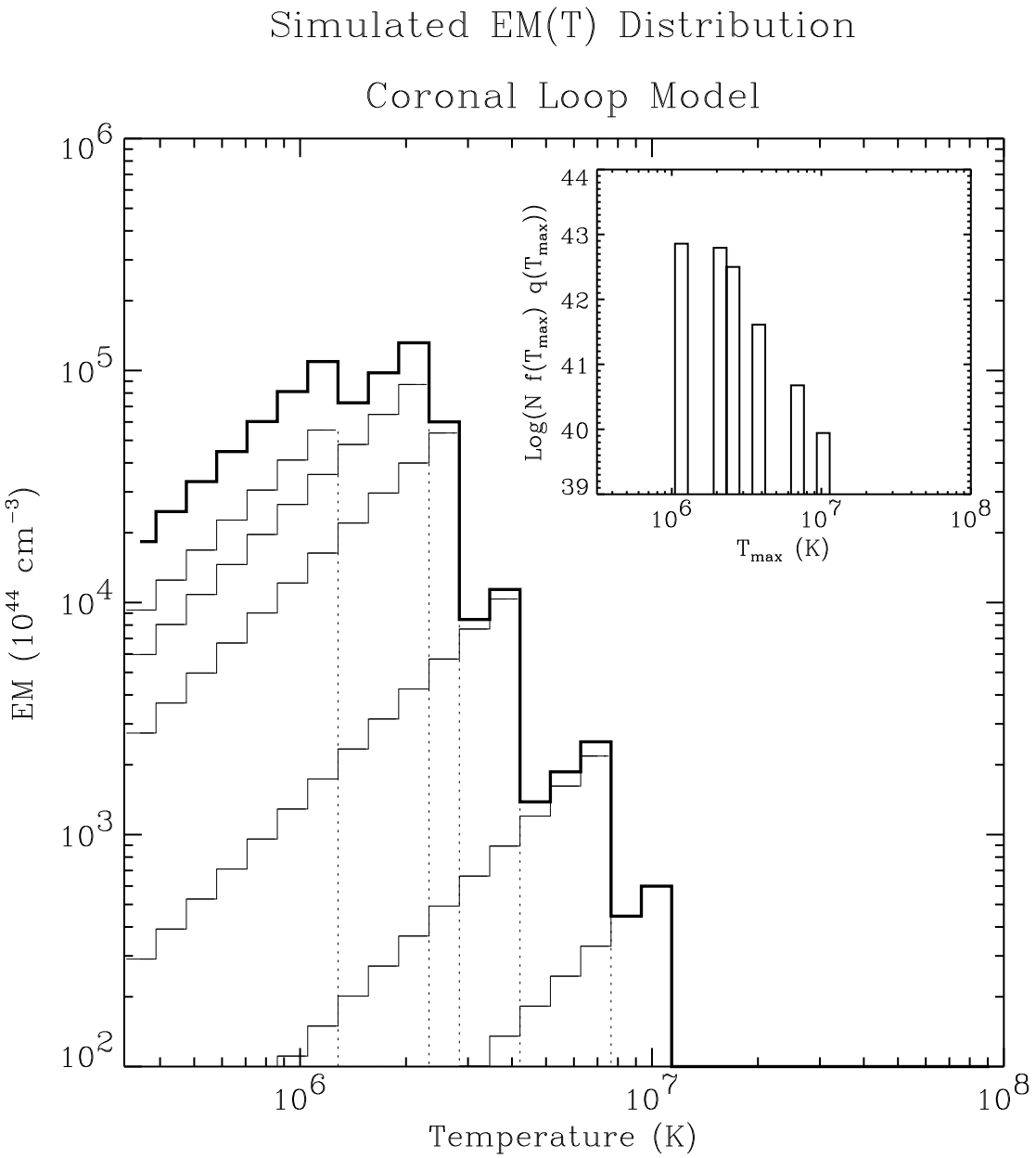
Simulated EM(T) Distribution
Coronal Loop Model
EM (10^{44} cm^{-3})
Temperature (K)
Log(N f(T_{max}) q(T_{max}))
T_{max} (K)

Fig. 1.—

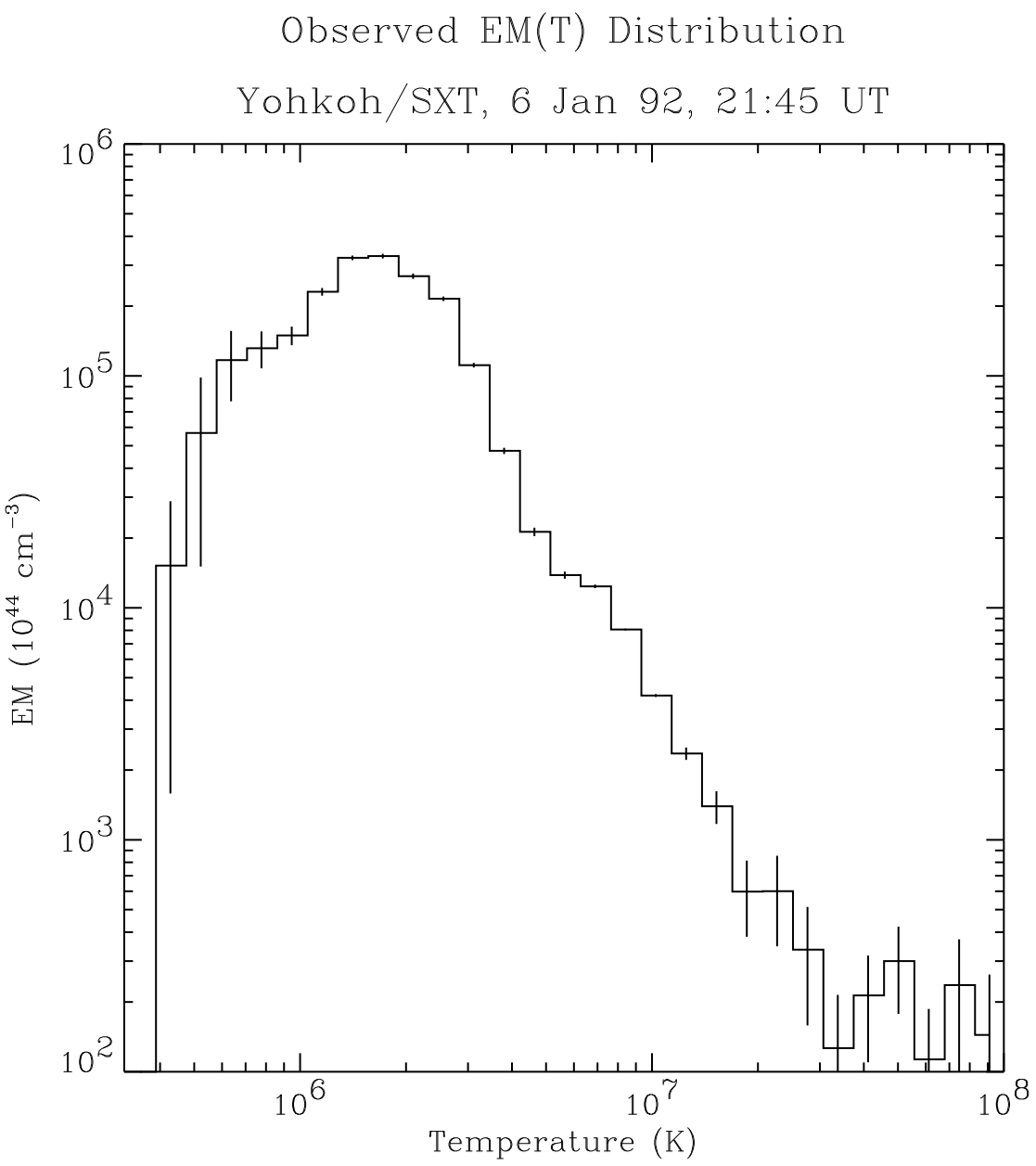
Observed EM(T) Distribution
Yohkoh/SXT, 6 Jan 92, 21:45 UT
EM (10^{44} cm^{-3})
10^6
10^5
10^4
10^3
10^2
10^6
10^7
10^8
Temperature (K)

Fig. 2.—

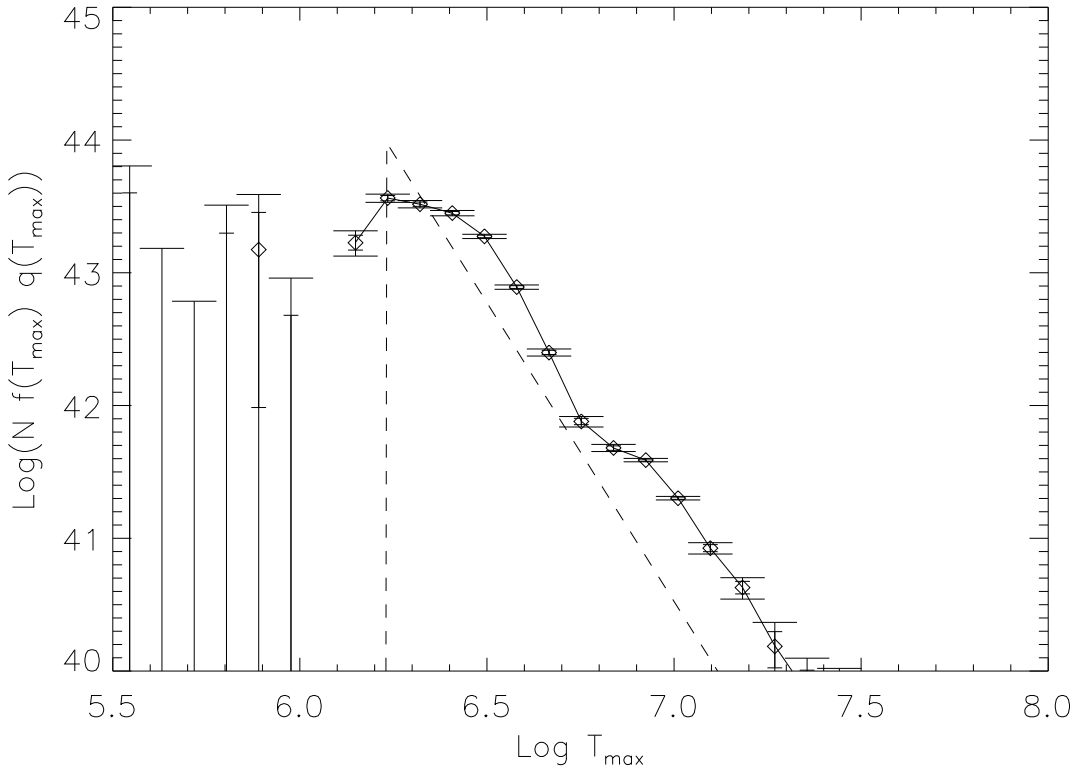

Fig. 3.—

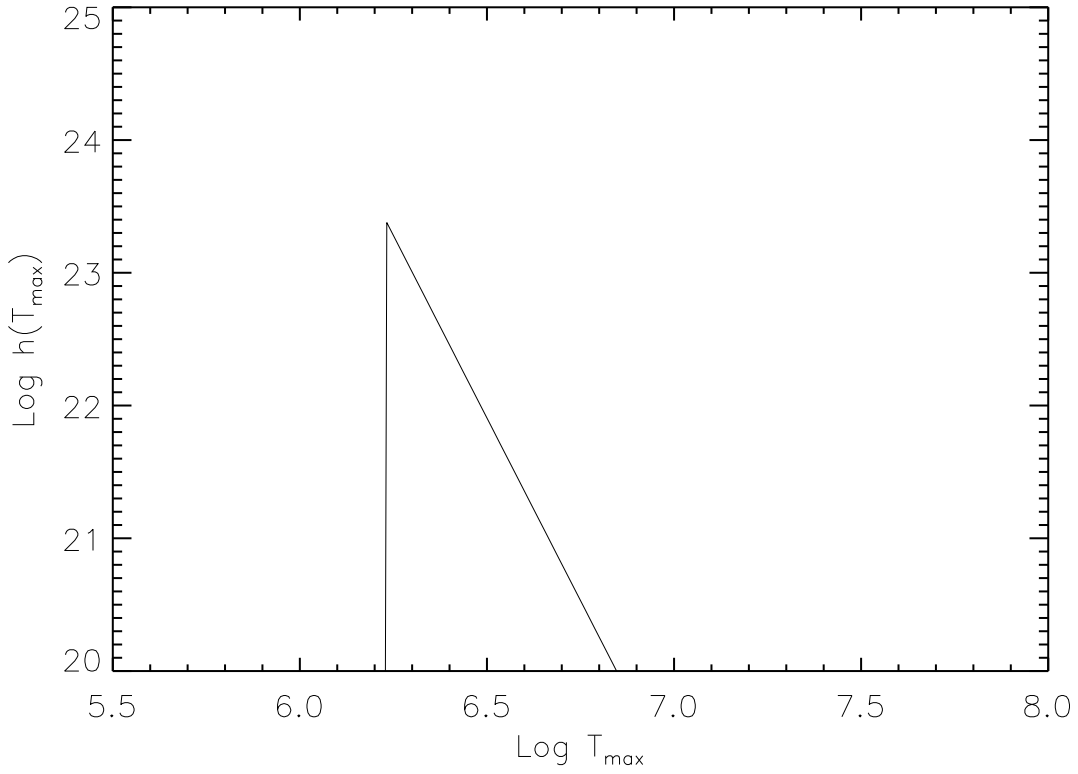

Fig. 4.—

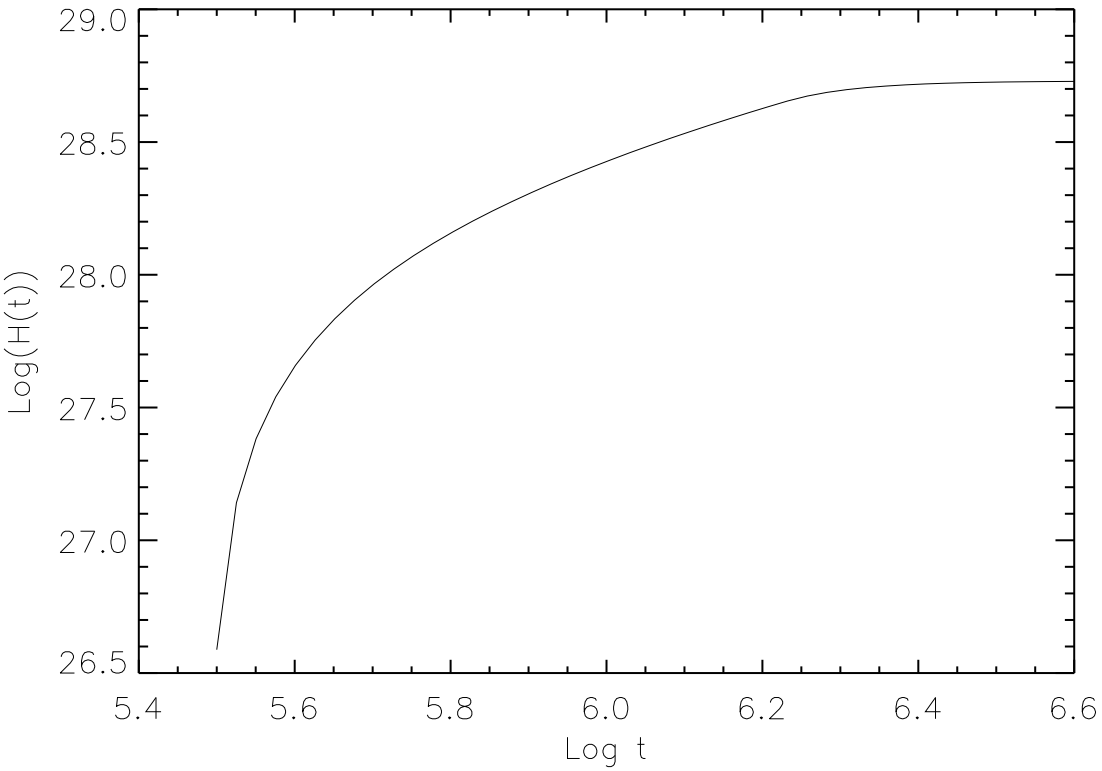

Fig. 5.—

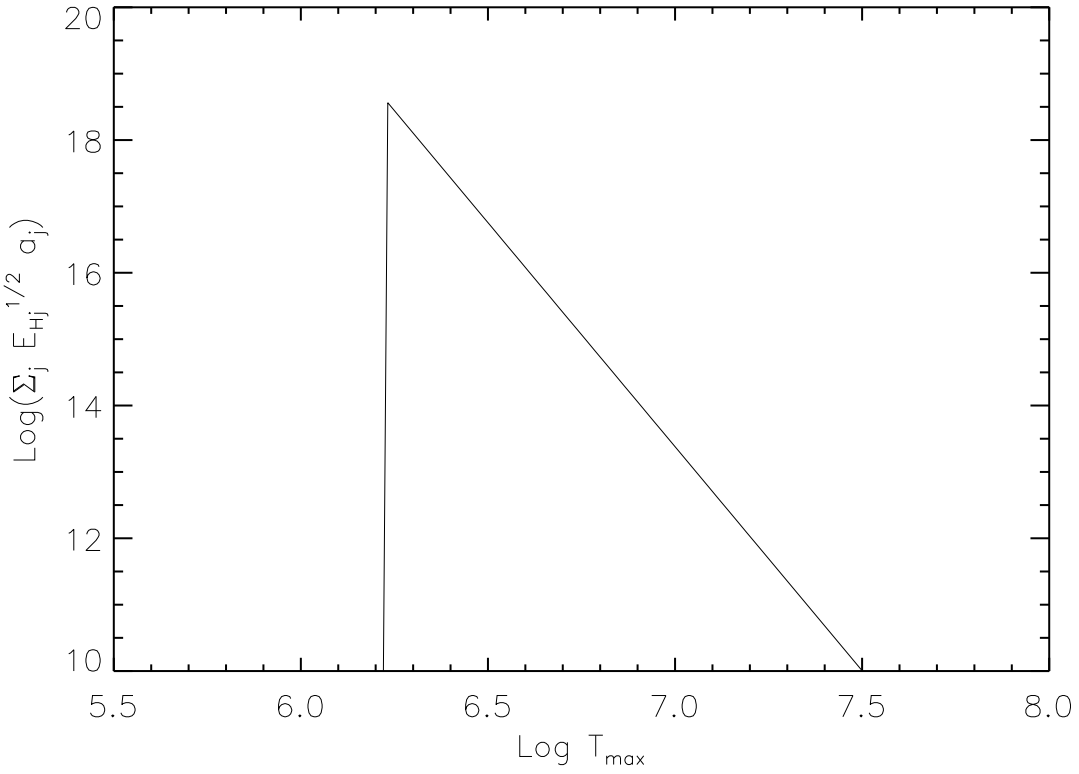

Fig. 6.—